

X-Ray diffraction study and die geometry effect on structural and mechanical characteristics of a nanosized severely deformed 6063 aluminum alloy

N. ȘERBAN*, D. RĂDUCANU, V. D. COJOCARU

Materials Processing and Ecometallurgy Department, Materials Science and Engineering Faculty, University „Politehnica” of Bucharest, Romania

Equal Channel Angular Pressing (ECAP) is the main Severe Plastic Deformation (SPD) technique for obtaining nanosized (NM) and ultrafine grained (UFG) materials, the advanced grain refinement obtained by SPD substantially enhancing microstructural and physicomechanical characteristics for the processed material. In our study, a commercial 6063 Al alloy was pressed at room temperature for nine passes using three different die geometries, the as-received and ECAP processed samples being considered for a series of structural and mechanical investigations. The specimens were firstly analyzed in OES and XRD tests. The Williamson-Hall method was applied for evaluating crystallite size and lattice strain. Samples were cut from each specimen and prepared for microstructural investigations (optical microscopy) and mechanical testing (compression and microhardness tests). Furthermore, the ECAP die geometry effects on structural and mechanical characteristics of severely deformed 6063 Al alloy were established.

(Received August 30, 2015; accepted September 9, 2015)

Keywords: Aluminum alloys, Severe plastic deformation, ECAP processing, XRD analysis, Williamson-Hall technique

1. Introduction

Advanced materials with submicrometer grain sizes were, in the last years, the main focus point for worldwide researchers and scientists. Conventionally, considering the associated crystallite size, these materials were classified as ultrafine grained (UFG) materials, with grain sizes between 100 nm and 1000 nm and nanomaterials (NM), having crystallite sizes smaller than 100 nm [1-3]. The properties of NM and UFG materials are superior to those of corresponding conventional coarse grained material; mechanical, microstructural and physical characteristics being significantly improved through the advanced grain refinement [4].

Transforming coarse grained materials into NM/UFG materials, involves imposing an exceptionally high strain in order to introduce a high density of dislocations and for these dislocations to subsequently rearrange in order to form an array of grain boundaries [5-8]. A particular set of techniques for the production of bulk nanostructured and UFG materials is based on severe plastic deformation (SPD), formally defined as those metal forming procedures in which a very high strain is imposed on a bulk solid without the introduction of any significant change in the overall dimensions of the solid, leading to exceptional grain refinement, with grain sizes mostly in the submicrometer or in the nanometer range [5]. Contrastive to classical deformation processes (forging, rolling, die-forging, extrusion etc.), the key benefit of SPD, with equal channel angular pressing (ECAP) as an emblematic technique, is that SPD involves inducing very

large strains in the processed material, without modifying the initial shape of the billet during deformation [6].

Since ECAP is also suitable for processing large billets, from the various SPD procedures, this is the most appealing technique, mainly because of its high potential in manufacturing materials for a variety of structural applications. This way, ECAP could be scaled up and used for industrial purposes, especially in processing advanced materials for the next generation [9-12]. In ECAP, severe grain refinement occurs together with the dislocation strengthening, significantly improving this way the mechanical behavior for the processed alloys [13-18].

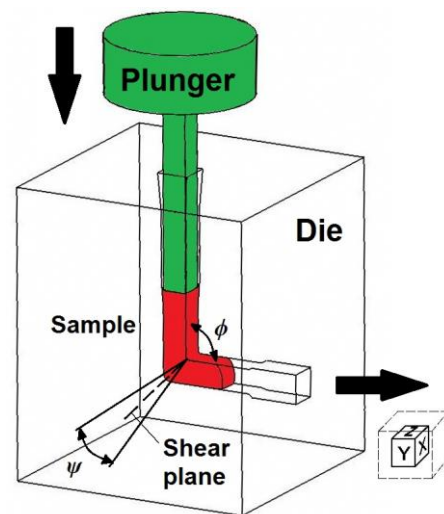


Fig. 1. ECAP concept showing the main technological elements

Equal channel angular pressing involves passing the billet (usually round or squared) throughout a die containing two intersecting channels identical in cross section. As shown in Fig. 1, the intersection angle is ϕ and a secondary angle of ψ sets the curvature from the outward intersection point of the channels [19]. In Fig. 1, the X, Y and Z planes denotes the transverse plane, the flow plane and the longitudinal plane, respectively. The material moves like a rigid body, the deformation being performed quasi-ideally by simple shear in a thin layer (a plane) at the intersection of the two channels of the die (the shear plane) [20]. Despite the introduction of a very intense strain the sample ultimately emerges from the die without experiencing any change in the cross sectional dimensions. Since the cross sectional area remains unchanged, the same sample may be pressed repetitively in order to attain exceptionally high strains and an advanced microstructure refinement [15]. By simply rotating the samples on each consecutive passage through the die, therefore by changing the shear plane and the shear direction, controlling the microstructure and texture for processed materials is made possible, therefore becoming possible to control their mechanical properties [16, 21]. In ECAP, four major processing routes are possible based on the sample rotation [9]. Route A is defined when the billet is not subjected to any rotation between passes. If the sample is alternately rotated 90° in opposite directions, after each passage through the die, then the deformation is performed following route B_A. Also, by rotating the sample after every pass 90° , but preserving the same direction, route B_C is established. Finally, a 180° billet rotation between passages defines the processing route C [22-25]. In this study, ECAP route B_C was used, as it was found to be the most effective for microstructural control and mechanical properties improvement [5, 8, 12, 26]. This technique can be applied to commercial pure metals and metal alloys, with FCC, BCC and HCP crystal structures, with coarse grains to fabricate ultrafine grained materials or nanomaterials with no porosity and superior mechanical properties, compared to the unprocessed materials [13-15].

2. Experimental details

Aluminum alloys are used in a wide range of industries, therefore they are considered to be vital materials for nowadays society, being preferred mainly because they are leading to the reduction of the product weight. However, aluminum was constantly highly demanded since the vast majority of its alloys are age hardenable and easily processable [27-30].

In our study, we examined a 6063 Al alloy, in the T1 condition (cooled from an elevated temperature shaping process and naturally aged), which is generally known as an architectural alloy. The chemical composition (wt. %) of the 6063 alloy used in the experiments was: Si 0.458, Mg 0.616, Fe 0.326, Cu 0.091, Mn 0.089, Zn 0.074, Ti 0.014, Pb 0.013, Ni 0.002, Cr 0.010, remainder Al. This chemical composition, for the investigated Al alloy samples, was established using a GNR *metal*-LAB 75/80V optical emission spectrometer (OES).

The ECAP specimens (with 60 x 9.6 x 9.6 mm initial dimensions) originated from a 120 mm round extrusion billet, industrially manufactured using a continuous casting and heat treating technology. Three ECAP processing dies [31] with ϕ , the intersection angle, being 90° , 100° and 110° respectively, were assayed for 6063 Al alloy processing. Secondary angle, ψ , was around 20° for all three cases. By using a 1.96 MN (200 tnf) hydraulic press, the specimens were pressed at ambient temperature for nine passes, at a pressing speed of 10 mm/s. The samples were rotated counter clockwise 90° after every pass, thereby applying the ECAP processing route B_C. As lubricant, graphite powder was used.

Samples taken from all specimens (as-received and ECAP processed 6063 Al alloy) were investigated in XRD (X-Ray Diffraction) tests for phase identification and Williamson-Hall analysis (evaluation of crystalline sizes and lattice strain). A PANalytical X'Pert PRO MPD diffraction system with copper anode ($K_{\alpha 1} = 1.54065 \text{ \AA}$), goniometry and proportional detector was used for these measurements.

Also, for evaluating the die geometry effect on structural and mechanical characteristics of ECAP processed 6063 Al alloy, multiple samples intended for metallography and mechanical investigations were taken. For the ECAP-ed samples, in order for the microstructure to be examined only in the flow plane, the cutting direction was parallel to the ECAP direction. All samples were hot mounted and each of them was subject to grinding and polishing. All specimens were etched for 20 seconds using Keller's reagent. The microstructure of the ECAP processed and also of the as-received material was investigated using optical microscopy (OLYMPUS BX60M). The as-received 6063 Al alloy and all ECAP processed samples were mechanically investigated in compression tests, using a mechanical testing machine INSTRON 3382. Compression samples were cut to cylindrical shape of $\varnothing 8 \times 12$ mm. Ultimate compression strength (σ_{UCS}), yield strength (σ_{YS}) and compression modulus (G) were obtained. Also, all samples were microhardness investigated using a WILSON-WOLPERT 401MVA equipment, the main testing parameters being a testing force of 100 gf (0.98 N) and a dwell time of 30 s.

3. Results and discussions

The as-received and ECAP processed material was subjected to XRD analysis for phase identification. The achieved diffraction patterns, showing the variation of the X-Ray intensity versus the diffraction angle 2θ , are given in Fig. 2, the acquired raw data being processed in Crystal Impact Match! using ICDD PDF-2 database. From this figure one can observe the compounds that were indexed and therefore, the phases identified for these XRD records, namely: Al, Al₂Fe₃Si₄, Al₄Cu₂Mg₈Si₇, Mg₂Si for the as-received material; Al, Al_{0.5}Fe₃Si_{0.5}, Al₄Cu₂Mg₈Si₇, Mg₂Si for nine passes ECAP-ed material using the 100° and 110° dies and Al, Al_{0.5}Fe₃Si_{0.5}, Mg₂Si for nine passes ECAP processed 6063 Al alloy using the 90° die, respectively.

The $\text{Al}_4\text{Cu}_2\text{Mg}_8\text{Si}_7$ compound was no longer indexed for the 90° die, mainly due to the severe fragmentation of secondary phase particles generated by the high imposed strain, correlated with this phase low ratio in the analyzed material. Also, one can observe that ECAP processing is leading to the stress-induced transformation of the initial $\alpha\text{-AlFeSi}$ phase, the $\text{Al}_2\text{Fe}_3\text{Si}_4$ compound from the as-received material being indexed as $\text{Al}_{0.5}\text{Fe}_3\text{Si}_{0.5}$ in the processed alloy, regardless of the ECAP die geometry.

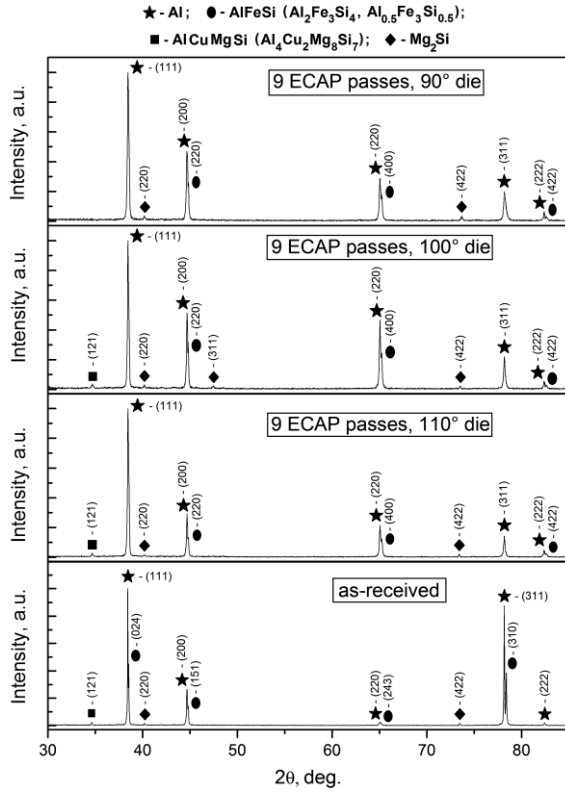


Fig. 2. X-Ray diffraction patterns of investigated 6063 Al alloy in the as-received condition and after 9 ECAP passes using the 90° , 100° and 110° dies, respectively

At the same time, the changes in diffraction peaks intensity are showing the preferential crystal orientation during ECAP processing, which is mainly driven by the shear plane interactions with the crystalline structure and the deformation texture and by the sample rotation system (the ECAP processing route) as well. Also, from Fig. 2, one can observe that the obtained diffraction peaks are wider for the ECAP-ed material, suggesting a smaller dimension of crystallites compared to the as-received state as a result of grain refining via ECAP processing.

Analyzing the XRD patterns for SPD processed 6063 aluminum alloy, crystallite size and microstrain can be evaluated using the Williamson-Hall technique, which is in fact Scherrer's equation corrected for considering also the lattice strain effect on diffraction peaks shape [32]:

$$FWHM \cdot \cos \theta = \frac{K \cdot \lambda}{D} + \varepsilon \cdot \sin \theta \quad (1)$$

where $FWHM$ is the full width at half maximum, θ is the diffraction peak position from the XRD pattern, K is the crystalline domain shape factor, λ is the X-ray wavelength, D is the crystallite size and ε is the microstrain.

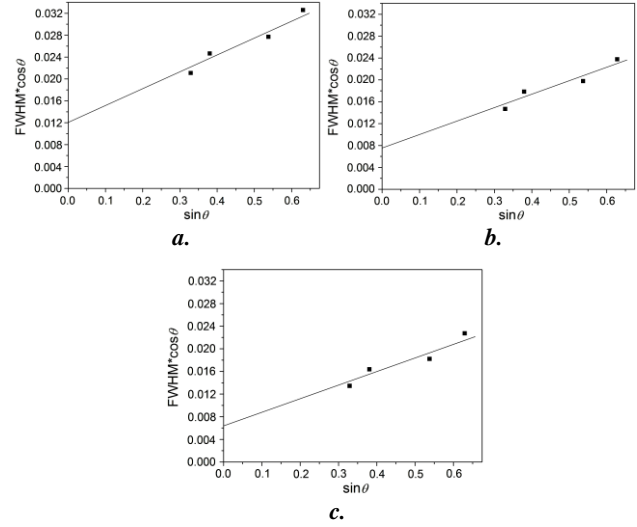


Fig. 3. Williamson-Hall plots for 9 passes ECAP processed 6063 Al alloy using the: a. 90° die; b. 100° die; c. 110° die

If Williamson-Hall plots ($FWHM \cdot \cos \theta$ versus $\sin \theta$) are drawn for the obtained diffraction patterns, then the microstrain can be estimated from the slope of variation and the crystallite size from the intersection with the vertical axis, as shown in Fig. 3. For plotting these diagrams, the XRD patterns were initially fitted in PeakFit (only the first four high intensity Al diffraction peaks) and the crystalline domains were considered as being relatively spherical. The data obtained from these plots are shown in Fig. 4, where the crystallite size and the microstrain are represented as a function of ECAP die geometry (the die channel angle). From this figure one can observe that the 90° ECAP die is the most effective for 6063 Al alloy microstructural refinement, the crystallite size increasing as ϕ , the intersection angle, increases (from about 13 nm for the 90° die, up to approximately 25 nm for the 110° die, which is nearly double).

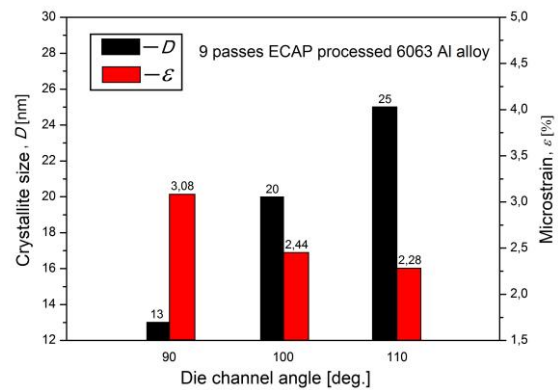


Fig. 4. Die geometry effect on crystallite size and microstrain for nine passes ECAP processed 6063 Al alloy

In case of microstrain, an inverse behavior was observed, this being maximum for the 90° ECAP die (approx. 3.10%), decreasing for the 100° die (approx. 2.45%) and reaching a minimum for the 110° die (of about 2.30%). This can be explained by considering the equivalent strain imposed on each passage through the die, which is higher when using a smaller die channel angle. Also, as the intersection angle ϕ , increases, the shear plane interactions with the crystalline structure and the deformation texture are becoming the decisive element for grain refining in ECAP.

The acquired optical microscopy images for all investigated samples are shown in Fig. 5 (for as-received and nine passes ECAP-ed material using the three die geometries). From this figure it can be seen that the microstructure of the as-received 6063 Al alloy shows a rough appearance, with large grains (an average size of about 100-150 μm) of dendritic aspect (or even polygonal equiaxed grains in patches) and with a secondary phase at grain boundaries, which is a typical continuous casting microstructure.

Considering also the obtained XRD results presented in Fig. 2, second phase particles were identified as one can see in Fig. 5a. Mg_2Si (magnesium-silicide) is usually found in Al-Mg-Si alloys either as a network of fine dispersed precipitates or as larger, relatively spherical particles [33]. AlCuMgSi is present in the unprocessed 6063 Al alloy as some acicular rod-shaped precipitates and the $\alpha\text{-AlFeSi}$ phase is described as having a Chinese letters characteristic morphology [34].

The ECAP processed samples (Fig. 5, b-d) are characterized by a microstructure with finished and homogeneous aspect, with refined, severely deformed grains, and also with crumbled and uniformly distributed secondary phase particles. Such microstructure was referred by other researchers [35, 36] as well and is described as bands of subgrains elongated and aligned with the shearing direction [37, 38].

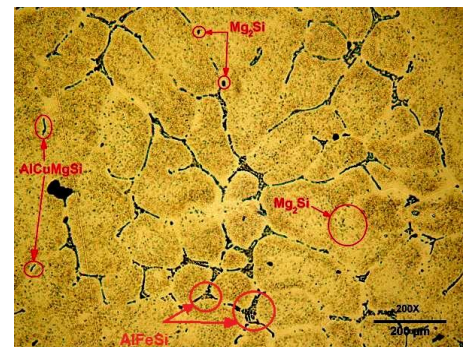
If the intersection angle ϕ decreases, we can observe a higher refining degree for the processed material, with smaller second phase particles, evenly distributed throughout the base metal, an adequate explanation for this fragmentation of secondary phase particles being given by considering the equivalent strain imposed in the ECAP processed samples.

Also, for a proper evaluation on the effect of ECAP die geometry on 6063 Al alloy mechanical behavior, the ECAP-ed material was compared to the unprocessed one in a series of mechanical investigations.

For all analyzed specimens, σ_{YS} (the yield strength), σ_{UCS} (the ultimate compressive strength), G (the compression modulus) and also the microhardness (HV0.1), were determined in compression and microhardness tests; the results recorded and computed during these mechanical investigations being shown in Figs. 6 and 7.

In Fig. 6, the engineering stress-strain diagrams for the as-received and the ECAP processed 6063 Al alloy, obtained through compression tests, are given. Also, from this figure one can observe a significant improvement in

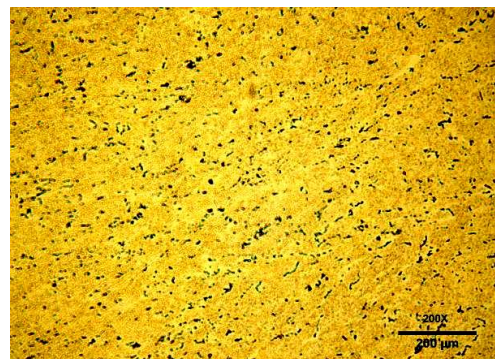
terms of mechanical properties for the ECAP-ed samples, due to the advanced grain refinement achieved within the processed material, the maximum effect being observed (as expected) when using the 90° ECAP die.



a.



b.



c.



d.

Fig. 5. Optical micrographs of investigated 6063 Al alloy (x200): a. as-received; b. 9 ECAP passes, 90° die; c. 9 ECAP passes, 100° die; d. 9 ECAP passes, 110° die

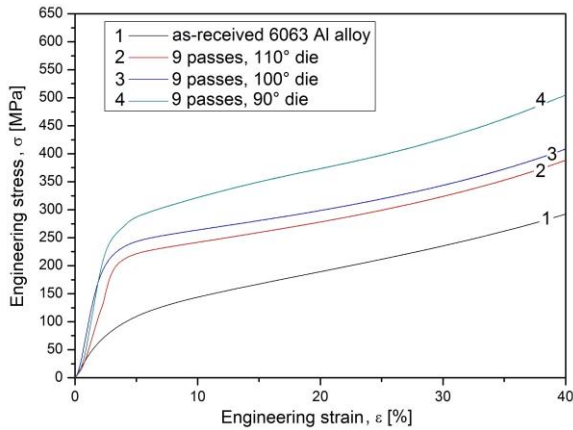


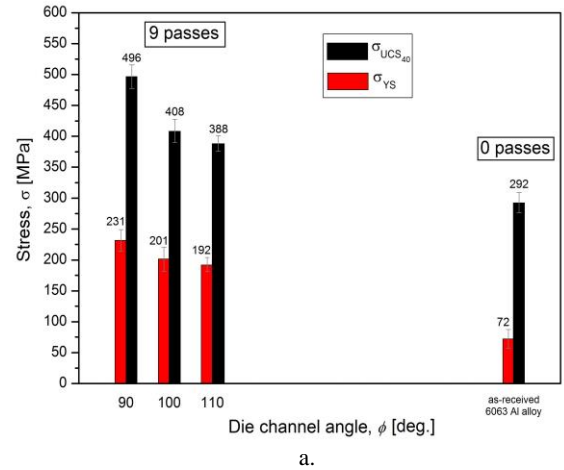
Fig. 6. Engineering stress-strain diagrams (compression tests) for the investigated 6063 Al alloy

Analyzing the data presented in Fig. 7a, one can observe an increase for the ultimate compressive strength (σ_{UCS}) of about 33% when using the 110° die (from 292 MPa for the as-received state up to 388 MPa after 9 ECAP passes), of approximately 40% for the 100° die (reaching 408 MPa after 9 passes) and of nearly 70% when using the 90° die (σ_{UCS} being 496 MPa after 9 ECAP passes). For the yield strength (σ_{YS}) the same behavior was observed, being recorded significant increases of more than 166% for the 110° die (from 72 MPa for the unprocessed material, up to 192 MPa), of approximately 179% for the 100° die (up to 201 MPa) and respectively of 221% for the sample processed using the 90° ECAP die (σ_{YS} being 231 MPa in this case).

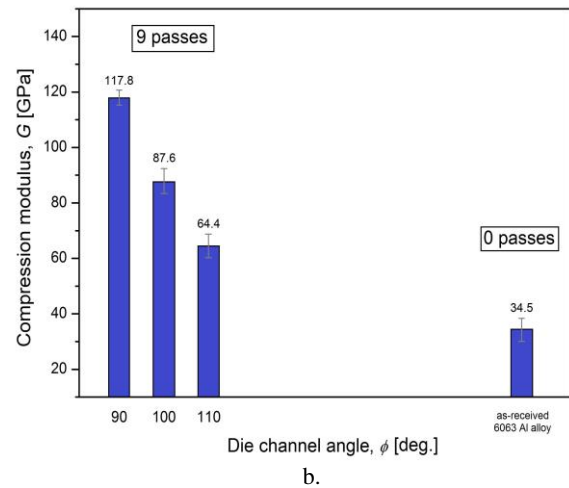
The compression modulus (G) registers an increasing of more than 86% after 9 ECAP passes using the 110° die (from 34.5 GPa, up to 64.4 GPa), of about 154% for the 100° ECAP die (up to 87.6 GPa after 9 passes) and of approximately 241% for the 90° die (up to 117.8 GPa for 9 passes ECAP processed 6063 Al alloy), as shown in Fig. 7b. As expected, the same behavior was also observed in case of microhardness; Fig. 7c showing an increasing of approximately 115% when using the 110° die (from 38.9 HV0.1 for the as-received material, up to 83.7 HV0.1 for 9 passes ECAP processed 6063 Al alloy), of approximately 128.5% for the 100° die (up to 88.9 HV0.1) and of more than 140% for the 90° ECAP die (up to 93.6 HV0.1).

In order to explain the observed behavior, two strengthening models are to be considered. The first one, described by [39], states that the necessary stress for inducing dislocation loops in a series of coarse grains, having the critical semicircle configuration, is establishing the plastic flow in a nanostructured material. The second strengthening model, referred by [40], describes the combined influence of two mechanisms in the course of heavy deformation of metals and metal alloys, namely grain boundaries strengthening as stipulated through the Hall-Petch equation and dislocation strengthening due to the occurrence of incidental dislocation boundaries having a low misorientation angle. Another possible deformation mechanism is different and more difficult to be proved; it implies no contributions of dislocations and no stress

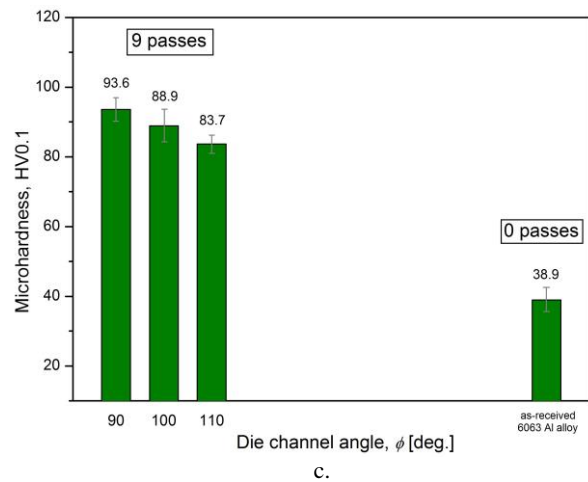
induced phase transformations [41]. In this case, a strange plastic deformation mechanism, considerably different from that of normal metallic materials acts: the deformation progresses by formation of giant faults, crystal lattice local disturbances at nanometer scale are possible, generating localized strain fields. This is a way to gain a dislocation free structure and to attain ultrastrength.



a.



b.



c.

Fig. 7. ECAP die geometry effect on 6063 Al alloy mechanical characteristics: a. yield strength and ultimate compressive strength; b. compression modulus; c. microhardness

4. Conclusions

In this study, we evaluated the ECAP die geometry effects on structural and mechanical characteristics of a severely deformed 6063 aluminum alloy. A detailed XRD analysis was conducted for phase identification and crystallite size and microstrain estimation via the Williamson-Hall method. The phases identified for the investigated material were Al, AlFeSi, AlCuMgSi and Mg₂Si, being found that ECAP processing is leading to the stress-induced transformation of the initial α -AlFeSi phase, regardless of the ECAP die geometry. The Williamson-Hall analysis highlighted the advanced grain refinement obtained after ECAP processing and showed a smaller crystallite size associated with a high microstrain value as the die channel angle decreases. It was found that the microstructure of the unprocessed 6063 Al alloy features a rough appearance, portrayed by coarse grains having a dendritic configuration and a second phase at grain boundaries, this being a typical continuous casting microstructure. In case of ECAP-ed specimens, the microstructure is distinguished by a finished appearance, with severely deformed, refined grains and a homogeneous distribution of crumbled second phase particles. Decreasing the die channel angle value, secondary phase particle size becomes smaller and its distribution is getting more and more uniform and also the material grain size is more finished. XRD analysis and optical microscopy studies showed that the 90° ECAP die is the most effective for 6063 Al alloy microstructural refinement and therefore is leading to superior mechanical properties. Considering the mechanical characteristics, significant increases were obtained via SPD, compared to the as-received 6063 Al alloy, the maximum effect being noted (as expected) for the 90° ECAP die. Increases for the ultimate compressive strength (σ_{UCS}) of nearly 70%, in yield strength (σ_{YS}) of 221%, for the compression modulus (G) of approximately 241% and for the microhardness of more than 140% were obtained after nine ECAP passes using the 90° die. It was shown that grain refining via SPD/ECAP processing results in significant enhancements of mechanical characteristics for 6063 Al alloy, such superior mechanical properties being highly desirable when manufacturing advanced materials for structural applications.

Acknowledgements

This work has been funded by the Sectoral Operational Programme Human Resources Development 2007-2013 of the Ministry of European Funds through the Financial Agreement POSDRU/159/1.5/S/134398.

References

- [1] R. Z. Valiev, Y. Estrin, Z. Horita, T. G. Langdon, M. J. Zehetbauer, Y. T. Zhu, *JOM* **58**, 33 (2006).
- [2] Y. Beygelzimer, V. Varyukhin, D. Orlov, B. Efros, V. Stolyarov, H. Salimgareyev, *Ultrafine Grained Materials II*, TMS, Warrendale PA (2002).
- [3] M. J. Zehetbauer, R. Z. Valiev, *Nanomaterials by Severe Plastic Deformation*, Wiley-VCH, Weinheim, Germany (2004).
- [4] V. D. Cojocaru, D. Răducanu, N. Șerban, I. Cinca, R. Șaban, *U. P. B. Sci. Bull. B Chem. Mater. Sci.* **72**, 193 (2010).
- [5] R. Z. Valiev, T. G. Langdon, *Prog. Mater. Sci.* **51**, 881 (2006).
- [6] R. Z. Valiev, R. K. Islamgaliev, I. V. Alexandrov, *Prog. Mater. Sci.* **45**, 103 (2000).
- [7] N. Șerban, N. Ghiban, V. D. Cojocaru, *JOM* **65**, 1411 (2013).
- [8] N. Șerban, V. D. Cojocaru, M. Buțu, *JOM* **64**, 607 (2012).
- [9] M. Furukawa, Y. Iwahashi, Z. Horita, M. Nemoto, T. G. Langdon, *Mater. Sci. Eng. A* **257**, 328 (1998).
- [10] Y. Iwahashi, Z. Horita, M. Nemoto, T. G. Langdon, *Acta Mater.* **45**, 4733 (1997).
- [11] N. Șerban, V. D. Cojocaru, M. Buțu, *U.P.B. Sci. Bull. B Chem. Mater. Sci.* **73**, 213 (2011).
- [12] J. Zrnik, S. V. Dobatkin, I. Mamuzic, *Metalurgija* **47**, 211 (2008).
- [13] C. J. L. Pérez, R. Luri, *Mech. Mater.* **40**, 617 (2008).
- [14] Y. Iwahashi, J. Wang, Z. Horita, M. Nemoto, T. G. Langdon, *Scripta Mater.* **35**, 143 (1996).
- [15] V. M. Segal, *Mater. Sci. Eng. A* **197**, 157 (1995).
- [16] Y. Iwahashi, Z. Horita, M. Nemoto, T. G. Langdon, *Acta Mater.* **46**, 3317 (1998).
- [17] M. Nemoto, Z. Horita, M. Furukawa, T. G. Langdon, *Met. Mater. Int.* **4**, 1181 (1998).
- [18] S. Ferrasse, T. Hartwig, R. E. Goforth, V. M. Segal, *Metall. Mater. Trans. A* **28**, 1047 (1997).
- [19] J. C. Werenskiold, H. J. Roven, *Mater. Sci. Eng. A* **410-411**, 174 (2005).
- [20] K. Nakashima, Z. Horita, M. Nemoto, T. G. Langdon, *Mater. Sci. Eng. A* **281**, 82 (2000).
- [21] K. Xia, J. Wang, *Metall. Mater. Trans. A* **32**, 2639 (2001).
- [22] S. L. Semiatin, D. P. Delo, E. B. Shell, *Acta Mater.* **48**, 1841 (2000).
- [23] L. Dupuy, J. J. Blandin, *Acta Mater.* **50**, 3251 (2002).
- [24] L. Olejnik, A. Rosochowski, *B. Pol. Acad. Sci.* **53**, 413 (2005).
- [25] S. Ferrasse, V. M. Segal, F. Alford, J. Kardokus, S. Strothers, *Mater. Sci. Eng. A* **493**, 130 (2008).
- [26] Z. Horita, M. Furukawa, M. Nemoto, T. G. Langdon, *Mater. Sci. Tech.* **16**, 1239 (2000).
- [27] H. T. Naeem, K. S. Mohammed, *Dig. J. Nanomater. Bios.* **8**, 1621 (2013).
- [28] R. Z. Valiev, D. A. Salimonenko, N. K. Tsenev, P. B. Berbon, T. G. Langdon, *Scripta Mater.* **37**, 1945 (1997).
- [29] M. Ai-bin, Y. Nishida, J. Jing-hua, N. Saito, I. Shigematsu, A. Watazu, *Trans. Nonferrous Met. Soc. China* **17**, 104 (2007).
- [30] H. T. Naeem, K. S. Mohammed, K. R. Ahmad, A. Rahmat, *Dig. J. Nanomater. Bios.* **9**, 1309 (2014).
- [31] N. Șerban, D. Răducanu, V. D. Cojocaru, A. Ghiban, *Adv. Mat. Res.* **1114**, 129 (2015).

- [32] U. Holzwarth, N. Gibson, *Nat. Nanotechnol.* **6**, 534 (2011).
- [33] A. F. M. Arif, S. S. Akhtar, A. K. Sheikh, *J. Fail. Anal. and Preven.* **9**, 253 (2009).
- [34] L. F. Mondolfo, *Aluminum alloys: structure and properties*, Butterworths, London, Boston (1979).
- [35] A. P. Zhilyaev, D. L. Swisher, K. Oh-ishi, T. G. Langdon, T. R. McNelley, *Mater. Sci. Eng. A* **429**, 137 (2006).
- [36] M. Reihanian, R. Ebrahimi, M. M. Moshksar, D. Terada, N. Tsuji, *Mater. Charact.* **59**, 1312 (2008).
- [37] E. A. El-Danaf, M. S. Soliman, A. A. Almajid, M. M. El-Rayes, *Mater. Sci. Eng. A* **458**, 226 (2007).
- [38] K. Oh-ishi, A. P. Zhilyaev, T. R. McNelley, *Mater. Sci. Eng. A* **410-411**, 183 (2005).
- [39] J. Lian, B. Baudelet, A. A. Nazarov, *Mater. Sci. Eng. A* **172**, 23 (1993).
- [40] N. Hansen, X. Huang, D. A. Hughes, *Mater. Sci. Eng. A* **317**, 3 (2001).
- [41] T. Saito, T. Furuta, J. H. Hwang, *Science* **300**, 464 (2003).

*Corresponding author: nicolae.serban@upb.ro
nicolae.serban@mdef.pub.ro